RevMexAA (Serie de Conferencias), **15**, 85–91 (2003)

STELLAR OUTFLOWS WITH NEW TOOLS: ADVANCED SIMULATIONS AND LABORATORY EXPERIMENTS

A. Frank,[1] A. Poludnenko,[1] T. A. Gardiner,[2] S. V. Lebedev,[3] and R. P. Drake[4]

RESUMEN

En esta contribución proporcionamos una breve reseña de nuevos resultados numéricos que describen la evolución de flujos grumosos además de nuevos estudios de chorros y vientos magnetizados. Además, reportamos un nuevo planteamiento para estudiar estos fenómenos: experimentos directos en el laboratorio. Avances recientes en el uso de aparatos de laboratorio de "alta densidad de energía" permiten ahora a los investigadores conducir experimentos de flujo de plasma escalables que son relevantes a los chorros astrofísicos hipersónicos y a las interacciones entre los choques y los grumos en el contexto de flujos circunestelares.

ABSTRACT

In this contribution we provide a brief overview of new numerical results describing the evolution of clumpy flows as well as new studies of magnetized winds/jets. In addition, we report on a new approach to studying these phenomena: direct laboratory experiments. Recent advances in the use of "high energy density" laboratory devices now allows researchers to produce scalable plasma flow experiments relevant to hypersonic astrophysical jets and shock-clump interactions in the context of circumstellar outflows.

Key Words: **H II REGIONS — ISM: JETS AND OUTFLOWS — STARS: MASS LOSS — STARS: PRE-MAIN SEQUENCE**

1. INTRODUCTION

The circumstellar environments of both young and evolved stars reveal a wide variety of outflow structures including collimated wind-blown bubbles and narrow jets. In addition, many of these structures appear highly heterogeneous indicating the underlying flows may be intrinsically clumpy. Understanding the nature of these flows is critical to the study of both young and evolved star evolution as the outflows contain information about the central mass-losing source and its surrounding environment. Much can be understood about fundamental processes at the extremes of stellar evolution by learning to read their traces off the surrounding outflows.

In addition to issues relating to the nature of the central sources, studying circumstellar environments can shed light on fundamental physics processes associated with extreme plasma environments. Circumstellar flows comprise natural laboratories rich in "multi-physics" phenomena (multiple physical processes operating simultaneously) . An understanding of astrophysical jets, to name one example, is likely to require advances in our understanding of ideal and resistive MHD, the nature of MHD instabilities, the nature of radiative flows in shocks and the dynamics of heterogeneous flows.

The complexity of outflows surrounding circumstellar environments, however, often limits our ability to construct theories which can both recover observed characteristics and extract critical evolutionary information on the central source. Unless one is visited by the same angelic intelligences as John Dyson, one is often forced to use numerical simulations to study stellar outflows. Luckily, advances in both numerical algorithms (adaptive mesh refinement (AMR) methods) and computational power (via parallel methods) have allowed numerical theorists to achieve greater levels of realism and, hopefully, allow them to isolate key behaviors that can *then* be understood more deeply through traditional analytical techniques.

Recently, a new approach to the study of complex multi-physics plasma environments has been introduced. High energy density laboratory experiments using experimental apparatus designed for the study of inertial confinement fusion (i.e., high intensity lasers and pulsed power machines) have recently shown considerable promise as a means of probing time-dependent plasma processes directly relevant to astrophysical environments.

In this contribution we provide a brief overview of a number of new studies concerning circumstellar flows which utilize high-resolution numerical simulations (via advanced algorithms) as well as laboratory

[1]Department of Physics and Astronomy, Laboratory for Laser Energetics, University of Rochester, USA.
[2]Department of Astronomy, University of Maryland, USA.
[3]The Blackett Laboratory, Imperial College, London, UK.
[4]Atmospheric, Oceanic, and Space Sciences, University of Michigan, USA.

experiments. Our results address issues related to radiative MHD jets and winds as well as the propagation of strong shocks through inhomogeneous media. Our description here is necessarily cursory and we refer the reader to more detailed published reports or ask their patience where these reports are in preparation.

2. YSO JETS, MOLECULAR OUTFLOWS AND MAGNETIC ENTRAINMENT OF H_2

Young stellar objects (YSO) have long been known to exhibit both hypersonic collimated jets and less collimated molecular outflows. Even after many years of study, however, it is still unclear what relation these two forms of outflow have to each other. Two competing scenarios which hold some favor are: jet-driven models where HH jets power the molecular outflows via prompt entrainment at the shock, and wide-angle winds from the star in which the jet may simply be an illusion due to the wind's density stratification (Lee et al. 2001). In this section we present new simulations of outflows driven by *magnetized* wide-angle winds. Magnetic stresses in the wind can considerably alter the nature of the wind-driven outflows leading to unification of jet-driven and wide-angle wind-driven models (Gardiner & Frank 2001). In addition we have found a new mechanism for the entrainment of fast H_2.

The environment in our study is initialized using a model of a collapsing, rotating, axially symmetric sheet (see Delamarter, Frank, & Hartmann 2000). The model parameters include a central mass $M_* = 0.21\,M_\odot$, a collapse radius $r_0 = 5.37 \times 10^{16}$ cm, a flattening parameter $\eta = 2.5$, a centrifugal radius $R_c = 4.28 \times 10^{14}$ cm, an infall mass flux $\dot{M}_i = 10^{-6}\,M_\odot\,\mathrm{yr}^{-1}$, and an ambient temperature of 10 K. As shown by Delamarter et al. (2000), under these conditions even purely hydrodynamic winds will be focused by the ram pressure and inertia of the flattened, infalling environment.

In these simulations the central wind has a mass-loss rate of $10^{-7}\,M_\odot\,\mathrm{yr}^{-1}$, a wind velocity of $200\,\mathrm{km\,s}^{-1}$, and a temperature of 10^4 K. The magnetic field in the wind is approximated as being purely toroidal. The strength of the magnetic field is set by fixing the parameter $\sigma = (V_m/V_\infty)^3$, where V_m is the Michel velocity and V_∞ is the asymptotic wind velocity. The angular variation of the wind density and magnetic field is parameterized in a way intended to mimic MHD wind collimation in a simple manner. The calculations presented here have $\sigma = 0.1$ and a pole-to-equator density contrast of 100 (see Gardiner & Frank 2001). The computational domain is cylindrically symmetric and measures 2400 AU along the z-axis and 375 AU in radius. This domain is resolved on a high-resolution grid of 6400×1000 grid cells.

Figure 1 shows the logarithm of the total density and ambient density for a steady central wind. The wind shock stagnates close to the outflow with wind material redirected into a dense jet along the outflow axis. While the wind begins with higher density on the poles the amplification of the magnetic field at the shock greatly enhances the collimation. At early stages in the evolution the post-shock flow is not in equilibrium in the azimuthal direction and the shock-amplified magnetic field drives the gas toward the axis (Garcia-Segura et al. 1999; Gardiner & Frank 2001). In addition, the wind material is also shock focused by the oblique wind shock at later stages in the simulation (Delamarter et al. 2000) with the resulting cylindrically converging flow redirected into a jet in a manner similar to the formation mechanism of Cantó, Tenorio-Tagle, & Różyczka (1988). The ambient material is swept up into a shell bounding the outflow. Thus, these simulations demonstrate how the combination of magnetic and inertial forces can produce both jet- and molecular outflow-like patterns from a magnetized wide-angle wind interacting with a density and ram pressure stratified environment (Ostriker 1997).

2.1. *Magnetic Entrainment of H_2*

Figure 2 shows the logarithm of total and ambient density for a time-variable wind. The wind velocity is varied sinusoidally with a 20 year period and a 50% amplitude. Given previous studies of time-variable winds, one might expect to find internal working surfaces in the wind with ambient material swept up into a shell bounding the outflow. In these outflows, however, we also find shells of ambient material interior to the wind cavity at the location of internal working surfaces. The physical mechanisms leading to the formation of these shells can be inferred from the finger-like structures of ambient material being drawn from the slipstream at the cavity boundary into the center of the outflow. On small scales, the wind and ambient material become mixed across the slipstream. The ambient material is drawn into the center of the outflow via large-scale motions associated with shock-amplified, toroidal magnetic fields. We note that smaller scale fingers can also be seen in the steady wind calculations indicating that an incipient instability may be present, which is activated by the pulsing.

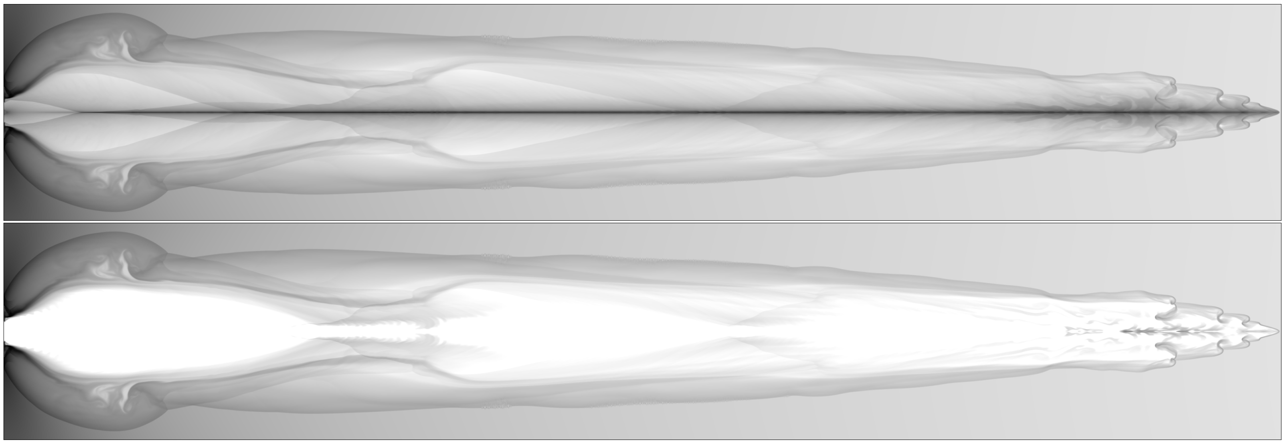

Fig. 1. Logarithm of the total density (*top*) and the ambient density (*bottom*) for a steady central wind. Number densities range from $900\,\mathrm{cm}^{-3}$ (*black*) to $4.32 \times 10^{8}\,\mathrm{cm}^{-3}$ (*white*).

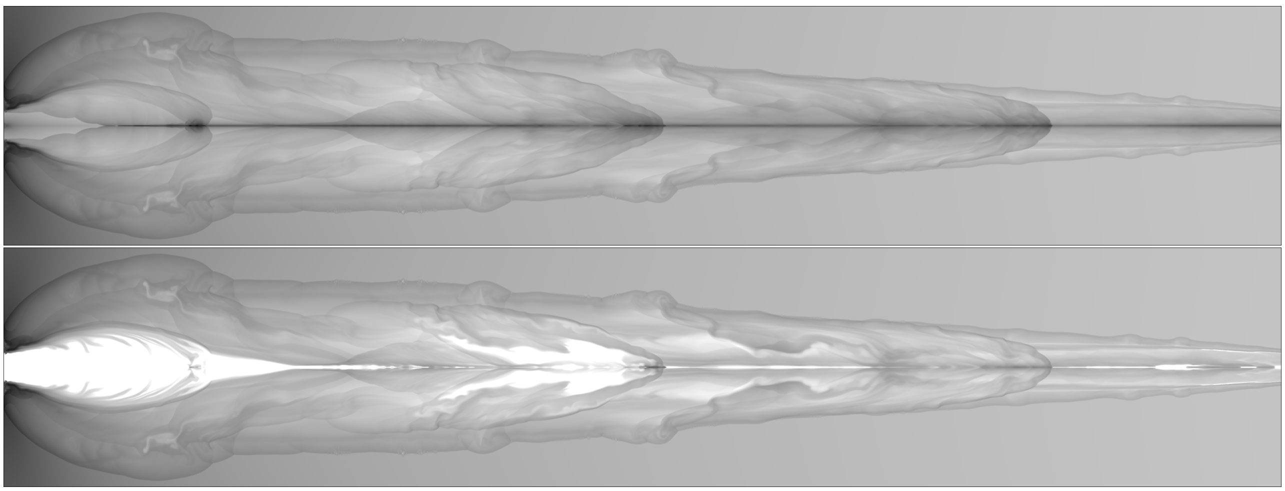

Fig. 2. Logarithm of the total density (*top*) and the ambient density (*bottom*) for a time-variable central wind. Number densities range from 800 (*black*) to $1.88 \times 10^{9}\,\mathrm{cm}^{-3}$ (*white*).

This *magnetic entrainment* offers a potential MHD mechanism for creating internal shells of fast moving molecular gas on short timescales. Internal molecular shells have been found to be important in explaining the presence of convex spurs in position-velocity (P-V) diagrams (Hubble wedges in mass-velocity (M-V) diagrams; see Lee et al. 2001, and references therein). A future paper will detail the observational properties of these outflow models.

3. HYPERSONIC FLOWS THROUGH CLUMPY MEDIA

Advances in high-resolution imaging have revealed many astrophysical environments to consist of highly inhomogeneous media. The presence of such clumpy mass distributions may have significant consequences for large-scale flows such as mass loss from both young and evolved stars, strong shocks propagating through interstellar clouds, and mass outflows from AGN. In each of these environments the momentum and energy exchange between the driver (the winds or interstellar shocks) and the ambient medium can be an important source of luminosity, non-thermal particles, mixing of enriched elements and, finally, turbulence. Thus the observations of clumpy flows point to a need for increased effort in understanding how inhomogeneous media can change fundamental astrophysical processes and affect the evolution of different astronomical environments.

The interaction of a shock wave with a clumpy medium has recently been analyzed in detail by Poludnenko, Frank, & Blackman (2002, PFB). This work differs from previous detailed investigations in which the shock interaction with only a single clump was studied (Klein, McKee, & Colella 1994). In PFB, systems with different numbers of clumps and different clump arrangements were simulated using an adaptive mesh refinement code. Figure 3 shows a single frame from a 14 clump simulation. The image is taken at a fairly early time after the global shock has passed through all the clumps (and is now propagating downstream to the right) but before the transmitted shocks have traversed any clump in the distribution. The interactions between clumps are, however, already apparent in the shapes of both bow shocks and wakes downstream of the first row of clumps.

Analytical arguments drawn from the simulations allowed PFB to identify two clumpy flow regimes. In the "interacting" regime, the evolution of individual clouds was strongly affected by their neighbors. As is well known (Klein et al. 1994), the behavior of individual shocked clumps in the adiabatic regime is dominated by compression and subsequent re-expansion perpendicular to the shock (flattening). When this expansion causes neighboring clumps to interact on a timescale shorter than the time for them to be destroyed by the post-shock flow the subsequent evolution is more appropriately described as a larger merged system, which then progresses towards turbulence.

In the non-interacting regime clumps are so widely separated that one can describe their evolution up to destruction in terms of a single shock-clump interaction. PFB found that clump distributions in the interacting regime showed more robust mixing between shock and clump material apparently due to stronger turbulent motions downstream. The enhanced mixing seen in PFB may have important consequences in astrophysical systems such as SNe and evolved stellar wind blown bubbles where processed elements in the clumps will be disbursed through the ISM. In the noninteracting regime clumps will evolve independently up to the time they are destroyed by the shock and post-shock flow.

PFB found that critical separation, $d_{\rm crit}$, perpendicular to the direction of shock propagation can be derived and expressed as

$$d_{\rm crit} = d_{\rm crit}(a_{\rm o}, v_{\rm s}, \chi, \gamma) \ , \qquad (1)$$

where $a_{\rm o}$, $v_{\rm s}$, and γ are the clump radius, shock speed and adiabatic index of the constituent gas. The parameter $\chi = \sqrt{n_{\rm c}/n_{\rm a}}$. When clumps are initially separated by a distance $d > d_{\rm crit}$ they will be destroyed before they interact. A similar quantity $L_{\rm crit}$ can be defined for the direction parallel to the direction of shock propagation. Expressions for $d_{\rm crit}$ and $L_{\rm crit}$ may be found in PFB.

To summarize, inhomogeneous flows will be in the interacting regime when initial clump distributions have average separations between clumps normal to the flow d such that $d < d_{\rm crit}$ and along the flow $L < L_{\rm crit}$. In the last section we use these results in describing simulations intended to explore the experimental design described in the previous section.

4. LABORATORY EXPERIMENTS

Advances in the development of intense lasers and pulsed power machines for inertial confinement fusion research has recently made plasma flow dynamics in astrophysically relevant parameter regimes accessible to laboratory investigation. The ability to "sculpt" targets and energy deposition in these machines with high precision opens the possibility of validating astrophysical numerical codes by comparing results from simulations with laboratory experiments. More important is the possibility that under certain circumstances the results from laboratory experiments can be directly compared to astrophysical systems through scaling arguments (Ryutov, Drake, & Remington 2000). In recent years high energy density experiments have been brought to bear on a variety of astrophysical topics ranging from blast wave stability to giant planet interiors (Remington et al. 1999). This new approach may prove particularly fruitful for studies of circumstellar flows with its emphasis on high Mach number shocks.

4.1. *Jet Experiments*

Astrophysical jets have been the subject of a number of recent investigations (Farley et al. 1999; Shigemori et al. 2000). A particularly promising approach appears to be the use of modified wire array pulse-power machines. Here we report on experiments in which a fast-rising current (reaching 1 MA in 240 ns) is applied to a conical array of fine metallic wires (Lebedev et al. 2002). The resistive heating rapidly converts the surface of the wires into a hot coronal plasma, which is then accelerated toward the wire array axis via the net $\mathbf{J} \times \mathbf{B}$ force. When the plasma reaches the axis, a conical standing shock is formed and the plasma is effectively redirected into an axial jet. Thus these experiments are able to explore the Cantó flows discussed in § 2.

Experimental runs were conducted using three different wire materials: aluminum (Al), stainless steel (Fe), and tungsten (W). The resulting jets for each of these materials are shown in Figure 4. Previous experiments have shown that the plasma velocity and mass flux driven off the wire array are

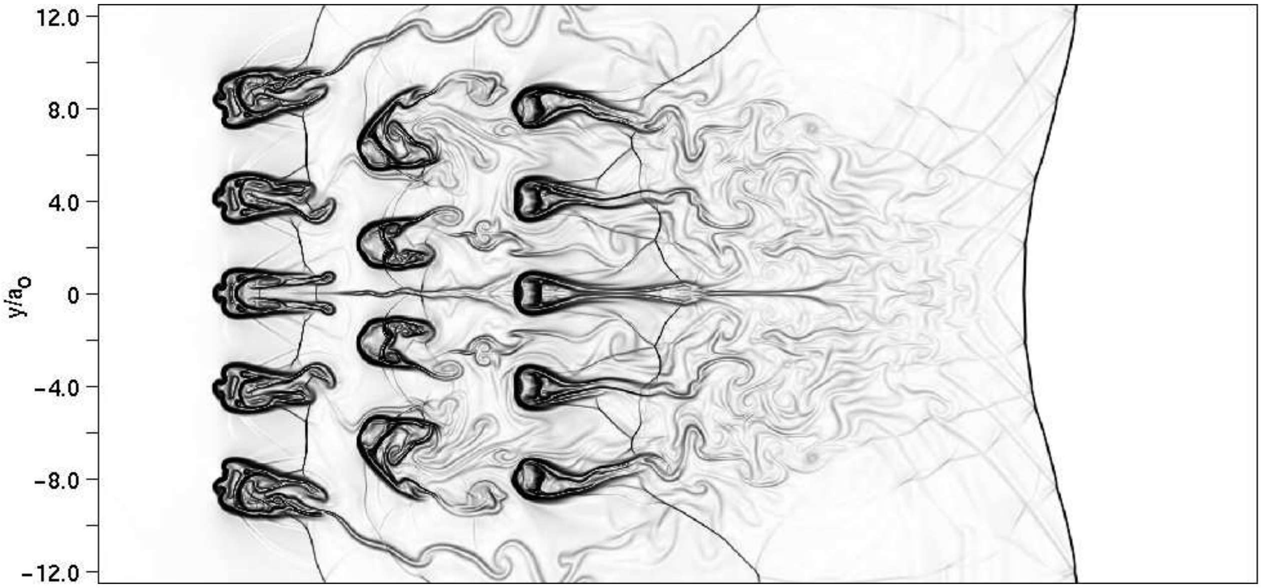

Fig. 3. AMR simulation of shocked clumpy flow: the shock has swept over clumps and is propagating off the grid. Note the strong clump-clump interaction downstream of the first clump row.

essentially insensitive to the material used. The energy loss through radiation, predominantly in lines, is, however, dependent on the atomic number (Post et al. 1977) . The radiative cooling rate can be estimated from a steady-state coronal equilibrium model, which indicates that cooling rates due to radiation increase with atomic number. This trend is consistent with the increased collimation and decreased jet radius observed to occur with increasing atomic number (base of Fig. 4). Using time-resolved imaging, the tungsten jet is found to have an axial velocity $V_z \sim 200\,\mathrm{km\,s^{-1}}$ and a radial expansion velocity $V_r < 7\,\mathrm{km\,s^{-1}}$. This provides an estimate of the internal Mach number of the jet, $M \sim V_z/V_r \sim 30$. Thus, the jets produced using W wires are hypersonic and radiative. As shown in Lebedev et al. (2002), all dimensionless parameters, including the cooling parameter $d_{\mathrm{cool}}/r_{\mathrm{j}}$ are in the appropriate regime. Only the Peclet number associated with thermal transport was lower than expected for astrophysical environments.

Of particular interest is the stability of "Cantó" cylindrically convergent flows and the resulting jets. To date, all hydrodynamic simulations that studied such flows assumed cylindrical symmetry. While such calculations demonstrated that Cantó flows would result in collimated jets, it was unclear if the collimation region and resulting jet would be stable. The Z-pinch experiments are directly relevant to this question. It is important to note that these experiments begin with significant perturbations since they utilize only 16 wires. To further examine the stability of such flows, two adjacent wires were removed and the experiments were repeated. For tungsten wires a well-collimated jet was still generated, though it emerged at an angle with respect to the wire-array axis. This indicates that the cylindrical symmetry condition can be relaxed if radiative losses are significant, a situation likely to occur in planetary and proto-planetary nebulae, as well as young stellar object jets such as those in § 2. Such a result, if borne out by further studies, demonstrates that these kinds of laboratory experiments can be directly relevant to unresolved astrophysical issues.

Having established the ability to create high Mach number radiative jets, the experimental testbed can be turned to examination of other jet dynamics issues. Recent images of HH objects in the Orion nebula (Bally & Reipurth 2002) have renewed interest in the properties of jets immersed in a crosswind. Jets can be deflected when exposed to crosswinds with high enough ram pressure. Recent experiments with the pulsed power testbed have explored such a situation. Irradiation of a thin plastic foil by X-rays created at the conical shocks can drive a crosswind via ablation. Fig. 4 shows images from such a crosswind experiment. In this figure the irradiated foil lies to the right of the jet. The jet direction has clearly been changed upon passing the foil. Note also the striations in the jet beam indicative of shocks forming due to interactions with the crosswind flow. While further investigations are required, at present it appears that the redirection occurs via collisional (i.e., fluid) interactions between

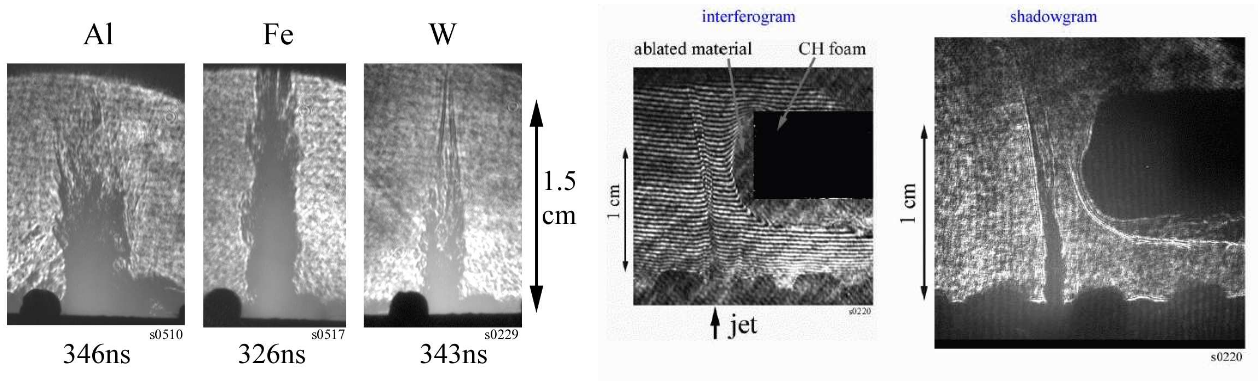

Fig. 4. Two laboratory astrophysical jet experiments: (*left*) laser probing images of plasma jets formed in (from left to right) aluminum, stainless steel, and tungsten wire arrays. These results show that the degree of collimation increases for elements with higher atomic number and, hence, higher rates of radiative cooling . (*Right*) Interferogram and shadowgraph of plasma jet deflection by crosswind. The crosswind forms via radiation induced ablation from a thin foil to the right of the jet.

the crosswind and the jet. The results of these experiments, along with comparison with analytical models (Cantó & Raga 1995) will be presented in an upcoming paper.

4.2. *Clump Experiments*

The interactions of multiple clumps with strong shock waves are another topic that can be explored with experiments. In a recent study, Poludnenko et al. (2003) explored a design for an experiment in which a blast wave driven by a pulsed power machine swept over a heterogeneous region of 200 carbon rods embedded in a low-density foam. The experimental goal was to articulate the gross changes in flow properties which would be driven by the presence of the clumps.

Adaptive mesh simulations of the experiment were carried out. The density contrast between the clumps and foam was $\eta = 40$ and the inter-clump spacing was small putting the clump distribution into the "interaction regime" defined in § 3: $d < d_{\rm crit}$, $L < L_{\rm crit}$. The results of the experiments showed that the shock speed was dependent on the presence of the clumps. Figure 5 shows plots of the shock position versus time for 3 simulations: clumps, no clumps, and no clumps but a background density equal to the average density in the presence of clumps. Our simulations showed that the shock speed in the presence of clumps lies between the no clump and average clump density cases. These results imply that shock dynamics in clumpy media are complex and that the use of average properties in studying clumpy media dynamics may not be justified.

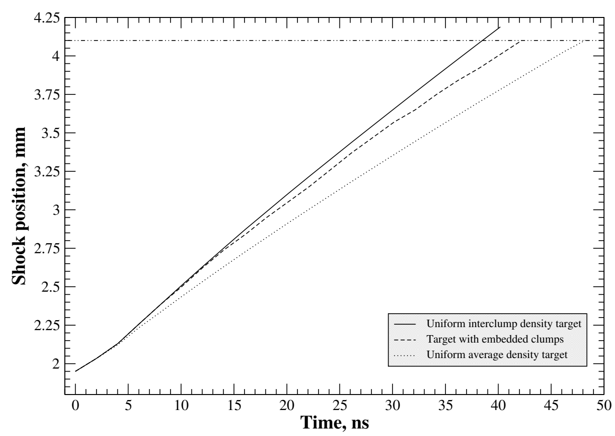

Fig. 5. Simulations of a clumpy flow laboratory experiment: shock position versus time for 3 simulations.

REFERENCES

Bally, J., & Reipurth, B. 2002, in Emission Lines from Jet Flows, eds. W. Henney, W. Steffen, A. Raga, & L. Binette, RevMexAA(SC), 13, 1
Cantó, J. & Raga, A. C. 1995, MNRAS, 277, 1120
Cantó, J., Tenorio-Tagle, G., & Różyczka, M. 1988 A&A, 192, 287
Delamarter, G., Frank, A., & Hartmann, L. 2000, ApJ, 530, 923
Farley, D. R., et al. 1999, Phys. Rev. Lett., 83, 1982
García-Segura, G., Langer, N., Różycka, M., & Franco, J. 1999, ApJ, 517, 767
Gardiner, T. A., & Frank, A. 2001, ApJ, 557, 250
Klein, R. I., McKee, C. F., & Colella, P. 1994, ApJ, 420, 213
Lebedev, S. V., et al. 2002, ApJ, 564, 113
Lee, C.-F., Stone, J. M., Ostriker, E. C., & Mundy, L. G. 2001, ApJ, 557, 429

Ostriker, E. 1997, ApJ, 486, 291
Poludnenko, A., Danneburg, K., Frank, A., & Drake, P. 2003, in preparation
Poludnenko, A., Frank, A., & Blackman, E. 2002, ApJ, 576, 832 (PFB)
Post, D. E., Jensen, R. V., Tarter, C. B., Grasberger, W. H., & Lokke, W. A. 1977, ADNDT, 20, 397
Remington, B., Drake, R., Takabe, H., & Arnett, D. 1999, Science, 284, 1488
Ryutov, D. D., Drake, R. P., & Remington, B. A. 2000, ApJS, 127, 465
Shigemori, K., et al. 2000, Phys. Rev. E, 62, 8838

R. Paul Drake: Atmospheric, Oceanic, and Space Sciences, University of Michigan, 2455 Hayward Street, Ann Arbor, MI 48109, USA.
Adam Frank and Alexei Poludnenko: Department of Physics and Astronomy, and Laboratory for Laser Energetics, University of Rochester, Rochester, NY 14610, USA (afrank@pas.rochester.edu).
Thomas Gardiner: Department of Astronomy, University of Maryland, College Park, MD 20742-2421, USA.
Sergey Lebedev: The Blackett Laboratory, Imperial College, London SW7 2BW, UK.